PNAS RESEARCH ARTICLE | NEUROSCIENCE

Fatty acid elongation by ELOVL6 hampers remyelination by promoting inflammatory foam cell formation during demyelination

Aida V. Garcia Corrales[a,1], Sanne G. S. Verberk[a,1], Mansour Haidar[a], Elien Grajchen[a], Jonas Dehairs[b], Sam Vanherle[a], Melanie Loix[a], Tine Weytjens[a], Pascal Gervois[c], Takashi Matsuzaka[d], Ivo Lambrichts[c], Johannes V. Swinnen[b], Jeroen F. J. Bogie[a,2], and Jerome J. A. Hendriks[a,2,3]

Edited by Lawrence Steinman, Stanford University, Stanford, CA; received January 23, 2023; accepted July 24, 2023

A hallmark of multiple sclerosis (MS) is the formation of multiple focal demyelinating lesions within the central nervous system (CNS). These lesions mainly consist of phagocytes that play a key role in lesion progression and remyelination, and therefore represent a promising therapeutic target in MS. We recently showed that unsaturated fatty acids produced by stearoyl-CoA desaturase-1 induce inflammatory foam cell formation during demyelination. These fatty acids are elongated by the "elongation of very long chain fatty acids" proteins (ELOVLs), generating a series of functionally distinct lipids. Here, we show that the expression and activity of ELOVLs are altered in myelin-induced foam cells. Especially ELOVL6, an enzyme responsible for converting saturated and monounsaturated C16 fatty acids into C18 species, was found to be up-regulated in myelin phagocytosing phagocytes in vitro and in MS lesions. Depletion of *Elovl6* induced a repair-promoting phagocyte phenotype through activation of the S1P/PPARγ pathway. *Elovl6*-deficient foamy macrophages showed enhanced ABCA1-mediated lipid efflux, increased production of neurotrophic factors, and reduced expression of inflammatory mediators. Moreover, our data show that ELOVL6 hampers CNS repair, as *Elovl6* deficiency prevented demyelination and boosted remyelination in organotypic brain slice cultures and the mouse cuprizone model. These findings indicate that targeting ELOVL6 activity may be an effective strategy to stimulate CNS repair in MS and other neurodegenerative diseases.

multiple sclerosis | fatty acid metabolism | remyelination | macrophage

Significance

Multiple sclerosis is a chronic autoimmune disease that results in demyelination and neurodegeneration of the central nervous system. Currently, there are no treatments that can effectively repair the damaged myelin sheath, and available therapies are limited to managing symptoms and slowing disease progression. Our study suggests that targeting elongation of very-long chain fatty acids protein 6 (ELOVL6) may provide an avenue for developing reparative therapies that could potentially restore function to damaged tissue. In this study, we investigate the potential of ELOVL6 as a therapeutic target for promoting remyelination in multiple sclerosis. Our findings demonstrate that ELOVL6 is significantly up-regulated in phagocytes in demyelinated lesions and that ELOVL6 deficiency induces a reparative phagocyte phenotype that promotes remyelination.

Multiple Sclerosis (MS) is a chronic inflammatory disease of the central nervous system (CNS) that affects over 2.3 million people worldwide (1). MS is the leading cause of neurologic disability in young adults, and available therapies are unable to stop neurological decline (1). The disease is characterized by the formation of demyelinating lesions containing abundant peripheral macrophages and CNS-derived microglia (2–4). These phagocytes display detrimental and beneficial functions in MS pathogenesis as they promote neuroinflammation, demyelination, and neurodegeneration, but also clear damaged myelin and produce neurotrophic factors, which facilitates remyelination (5, 6).

Ample evidence indicates that the intracellular lipid load determines the inflammatory and reparative properties of phagocytes in demyelinating lesions. Initially, myelin uptake skews phagocytes toward a reparative phenotype, accompanied by the production of neurotrophic factors (2, 7–9). However, sustained internalization of myelin leads to the formation of inflammatory foamy phagocytes that hinder CNS repair (10). Our recent study revealed that this inflammatory shift is directed by stearoyl-CoA desaturase-1 (SCD1), an enzyme responsible for the desaturation of saturated fatty acids (SFA) into monounsaturated fatty acids (MUFAs) (10). SCD1-derived MUFAs induce inflammatory foam cell formation by impairing ATP-binding cassette transporter A1 (ABCA1)-mediated cholesterol efflux. Importantly, pharmacological inhibition and genetic deficiency of SCD1 reduced the phagocyte lipid load and neuroinflammation, and promoted remyelination in in vivo models of MS. To date, however, the fatty acid-containing lipid species and downstream signaling cascades that underlie the impact of SCD1 on the inflammatory, reparative, and metabolic properties of phagocytes remain unclear.

Fatty acid elongation and desaturation reactions dynamically drive the cellular lipidome during homeostasis and disease (11). In this study, we show that the expression of ELOVL6 is highly increased in foamy macrophages and microglia in vitro and in MS lesions. Genetic deficiency of *Elovl6* reduced the intracellular accumulation of lipids, promoted ABCA1-mediated cholesterol efflux, and increased the expression of neurotrophic factors in myelin-containing phagocytes. Accordingly, phagocyte-specific deficiency of *Elovl6* improved remyelination and metabolic dysregulation in the cuprizone model. Finally, guided by lipidomics analysis, changes

The authors declare no competing interest.

This article is a PNAS Direct Submission.

[1]A.V.G.C. and S.G.S.V. contributed equally to this work.

[2]J.F.J.B. and J.J.A.H. contributed equally to this work.

[3]To whom correspondence may be addressed. Email: jerome.hendriks@uhasselt.be.

This article contains supporting information online at https://www.pnas.org/lookup/suppl/doi:10.1073/pnas.2301030120/-/DCSupplemental.

Published September 5, 2023.

in de novo sphingosine synthesis were found to underlie the impact of *Elovl6* deficiency on the metabolic and reparative phenotype of foamy macrophages. Collectively, our findings emphasize the significant role of fatty acid elongation in regulating phagocyte function within the CNS, which may have important therapeutic implications for multiple sclerosis (MS) and other neurodegenerative diseases.

Results

Myelin Internalization Increases ELOVL6 Expression in Phagocytes. To date, seven elongases have been identified in mammals (ELOVL1-7), each exhibiting a distinct substrate specificity (12–14). To determine whether myelin internalization alters the expression of *Elovl1-7* in phagocytes, qPCR was performed on mouse bone marrow-derived macrophages (BMDMs) treated with myelin for a short (24 h, Mye^{24}) or prolonged (72 h, Mye^{72}) period, corresponding to reparative and inflammatory foamy macrophage subsets, respectively (7) (Fig. 1*A*). Here, we found that prolonged myelin exposure increased the expression of *Elovl6* (Fig. 1*B*). Other elongases showed transcript levels on the lower detection limit for *Elovl2*, *3*, and *4* and decreased expression of *Elovl1* and *Elovl7* in myelin-loaded macrophages. Liquid-chromatography-electrospray ionization tandem mass spectrometry (LC-ESI/MS/MS) analysis further demonstrated a reduced C16/C18 elongation ratio in macrophages upon internalization of myelin, in particular after prolonged exposure to myelin (Fig. 1*C*). Given that ELOVL6 controls the elongation of C16 fatty acids (FAs), the latter finding supports the notion that myelin internalization increases ELOVL6 activity, likely through increasing its abundance (*SI Appendix*, Fig. S1 *A* and *B*). Additionally, within active human MS lesions, characterized by demyelination (PLP^-) and myelin-containing phagocytes (ORO^+, $HLA\text{-}DR^+$) (Fig. 1*D*), $CD68^+$ macrophages and microglia showed a marked increase in ELOVL6 levels (Fig. 1*E*). Specifically, the number of ELOVL6-expressing CD68+ phagocytes was elevated in the lesion center as compared to the lesion rim and NAWM (Fig. 1 *F* and *G*). ELOVL6 was not detectable in remyelinated lesions. Given that phagocytes in the lesion center contain abundant intracellular myelin remnants (10), these findings are consistent with prolonged myelin accumulation inducing *Elovl6* expression in vitro (Fig. 1*B*). Alongside foamy macrophages, ELOVL6 was also expressed by oligodendrocytes but not by astrocytes (*SI Appendix*, Fig. S1*C*), indicating a multicellular role of this enzyme in brain homeostasis and disease. Collectively, these results show that intracellular accumulation of myelin increases the expression and activity of ELOVL6 in phagocytes in MS lesions.

***Elovl6* Deficiency Promotes the Intracellular Processing of Myelin-Derived Lipids and the Induction of a Reparative Phagocyte Phenotype.** Having established that ELOVL6 expression and activity are enhanced in foamy macrophages, we next determined whether ELOVL6 impacts the metabolic phenotype of macrophages by analyzing the uptake, intracellular processing, and efflux of myelin-derived lipids. To this end, BMDMs were cultured in vitro from wildtype (Wt) and *Elovl6*-deficient ($Elovl6^{-/-}$) mice, and exposed to myelin to obtain foamy macrophages (Fig. 2*A*). $Elovl6^{-/-}$ BMDMs showed absence of ELOVL6 with unaffected viability (*SI Appendix*, Fig. S2 *A, B*). While *Elovl6* deficiency did not impact the uptake of myelin debris (Fig. 2*B*), $Elovl6^{-/-}$ BMDMs showed a reduced abundance of neutral lipids when compared to Wt macrophages (Fig. 2*C*). Additionally, the number of lipid droplets (LDs), which generally contain the bulk of neutral lipids in lipid-loaded phagocytes, were significantly decreased in $Elovl6^{-/-}$ BMDMs, as analyzed by transmission electron microscopy (TEM), Oil red O (ORO) staining, and fluorescent staining of PLIN2 and BODIPY493/503 (Fig. 2 *D*–*G*). Together, these data indicate enhanced overall neutral lipid processing in *Elovl6*-deficient phagocytes. Next, since cholesterol is a major constituent of lipid droplets, intracellular concentrations of cholesterol esters (CE) were determined. Lack of *Elovl6* reduced the intracellular levels of total (TC) and esterified cholesterol (EC), without affecting the amount of free cholesterol (FC) (Fig. 2*H*). Notably, reduced cholesterol levels were closely associated with an increased abundance of the cholesterol transporter ABCA1 and enhanced ABCA1-mediated cholesterol efflux in $Elovl6^{-/-}$ BMDMs exposed to myelin (Fig. 2 *I* and *J*). Absence of *Elovl6* did not affect ABCG1 levels and ABCG1-mediated cholesterol efflux (*SI Appendix*, Fig. S2 *C* and *D*). Collectively, these findings show that *Elovl6* deficiency promotes cellular processing and ABCA1-mediated efflux of myelin-derived lipids by foamy macrophages.

Impaired lipid handling and subsequent accumulation of myelin-derived cholesterol and lipid droplets in macrophages and microglia underlies the induction of a disease-promoting phagocyte phenotype in demyelinating disorders (10, 15, 16). Since absence of *Elovl6* reduced intracellular cholesterol and LD levels in BMDMs in vitro (Fig. 2), we next determined whether *Elovl6* deficiency counteracts the inflammatory phenotype associated with prolonged intracellular myelin accumulation. Stimulation of myelin-treated BMDMs with the inflammatory stimulus lipopolysaccharide (LPS) showed that *Elovl6* deficiency reduces the expression of interleukin 6 (*Il6*) and the secretion of IL-6, IL-13, and CXCL10, but does not affect the expression or secretion of other measured inflammatory mediators (*SI Appendix*, Fig. S2 *E* and *F*). Interestingly, myelin-treated $Elovl6^{-/-}$ BMDMs showed an increased expression of neurotrophic factors such as insulin growth factor 1 (*Igf1*), tumor growth factor β (*Tgfb1*), and ciliary neurotrophic factor (*Cntf*) (Fig. 2*K*). Taken together, these findings show that *Elovl6* deficiency skews myelin-laden macrophages toward a less-inflammatory, reparative phenotype.

De Novo Sphingosine Synthesis Is Up-Regulated in $Elovl6^{-/-}$ Macrophages. To define the impact of *Elovl6* deficiency on the metabolic phenotype of phagocytes, alterations in the lipidome of myelin-treated Wt and $Elovl6^{-/-}$ BMDMs were examined using LC-ESI/MS/MS (Fig. 3*A*). As expected, $Elovl6^{-/-}$ deficiency increased the ratio of C16:C18, but not the C18:C20 or C20:C22 ratios in BMDMs, indicating overall lower conversion of C16 FAs into C18 FAs in cells (Fig. 3*B*). Next to elongation, *Elovl6* deficiency also altered the desaturation status of major FA-containing lipid species (Fig. 3*C*), with glycerides and phospholipids showing increased and cholesterol esters and sphingolipids showing decreased SFA:MUFA ratios. Thus, Elovl6 indirectly controls desaturation of specific lipids. Alongside changes in elongation and desaturation, CE levels were reduced in $Elovl6^{-/-}$ BMDMs (*SI Appendix*, Fig. S3*A*), which confirms our findings showing a reduced presence of neutral lipid-containing lipid droplets in these cells (Fig. 2). Further, several sphingolipid classes, including sphingomyelins (SM), dihydroceramides (DCER), and hexosylceramides (HexCER) were increased in untreated and myelin-treated $Elovl6^{-/-}$ macrophages (Fig. 3 *D* and *E* and *SI Appendix*, Fig. S3*B*), indicating enhanced de novo sphingolipid synthesis in *Elovl6*-deficient BMDMs. To identify biological processes associated with changes in the lipidome of $Elovl6^{-/-}$ macrophages (*SI Appendix*, Fig. S3 *A–I*) lipid ontology (LION) enrichment analysis was applied (17). Changes in intracellular and secreted lipids from untreated $Elovl6^{-/-}$ BMDMs and myelin-treated $Elovl6^{-/-}$ BMDMs could be linked to several significantly enriched LION terms, including biophysical

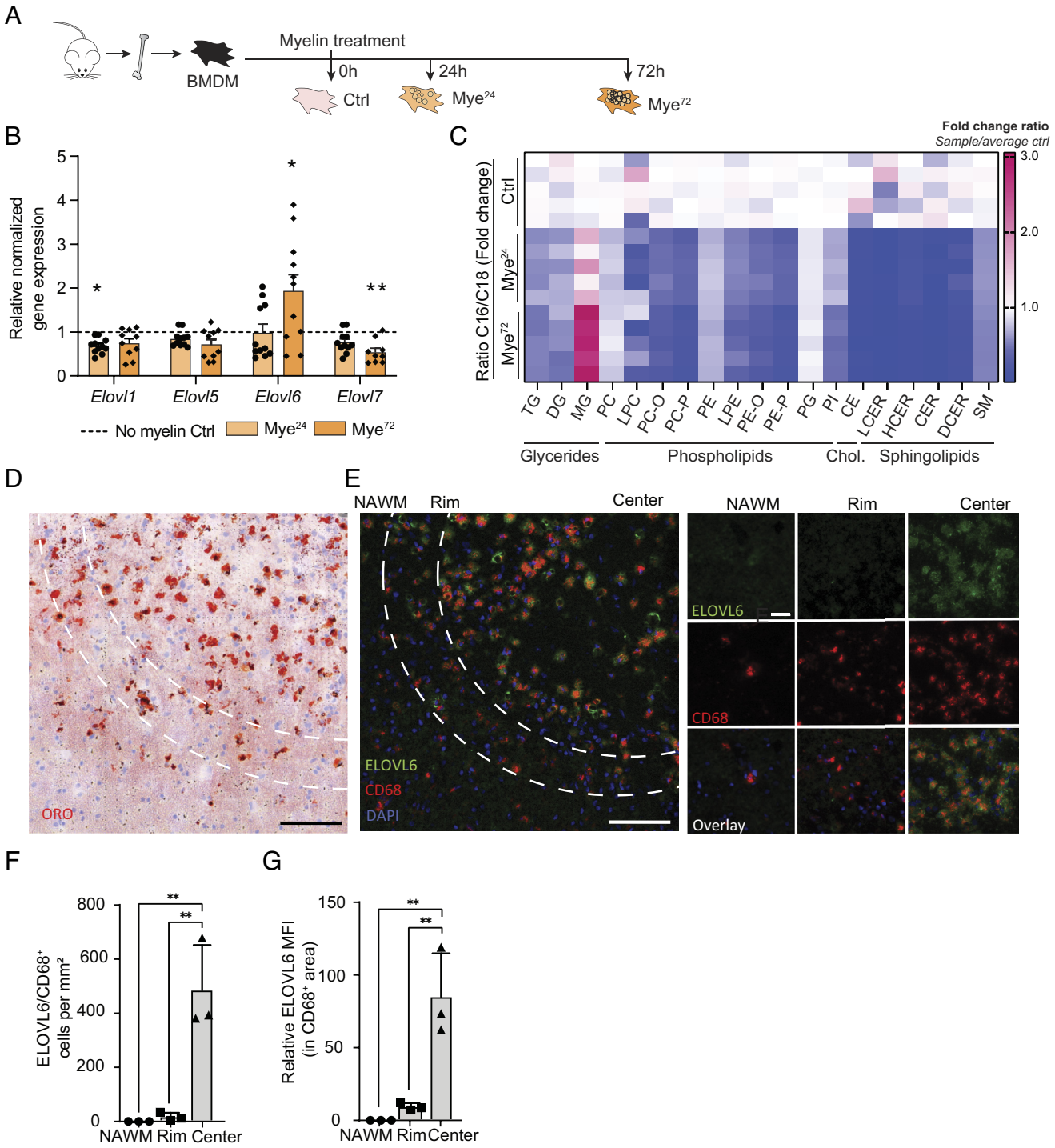

Fig. 1. Myelin internalization increases ELOVL6 expression in phagocytes. (*A*) Bone marrow-derived macrophages (BMDMs) were left untreated (Ctrl) or treated with acute exposure (24 h, Mye^{24}) or with sustained exposure (72 h, Mye^{72}) to 100 μg/mL myelin. (*B*) Gene expression of ubiquitous ELOVLs in 24-h and 72-h myelin-treated BMDMs (N = 12 wells per condition) relative to untreated BMDMs (dashed line). (*C*) Ratio of C16/C18 lipids as determined by ESI-MS/MS–based lipidomics analysis of 24-h and 72-h myelin-treated BMDMs relative to untreated BMDMs (Ctrl) (N = 5). LCER = LacCER, HCER = HexCER. (*D*) Oil red O (ORO) staining on active human post-mortem lesions indicating the lipid-rich lesion center. (Scale bar: 100 μm.) (*E*) Immunohistochemical (IHC) staining for ELOVL6 (green) and CD68 (Red) on a consecutive lesion slice highlighting ELOVL6 in CD68$^+$ phagocytes in the lesion center. (Scale bar: 100 μm, zoomed Scale bar: 50 μm.) (*F*) Quantification of ELOVL6$^+$ CD68$^+$ macrophages in normal-appearing white matter (NAWM), the rim and center of the active MS lesion (N = 3 lesions from three different donors). (*G*) Mean fluorescent intensity (MFI) of ELOVL6-signal within CD68$^+$ cells in NAWM, and the rim and center of an active lesion. All data are represented as mean ± SEM. *$P < 0.05$, ** and $P < 0.01$, unpaired Student's *t* test (*A*), one-way ANOVA (*F*–*G*).

properties (intrinsic curvature, lateral diffusion, and transition temperature), cellular components (endosome/lysosome, ER, and mitochondrion), and molecular components (fatty acids with 16 and 22 carbons) (*SI Appendix*, Figs. S4 *A*–*D* and S5 *A* and *B*). In accordance with our lipidomics analysis, lipid ontology analyses demonstrated an increase in sphingolipids in cells and medium, with specific enrichment in SM, HexCER, and sphingosines upon myelin treatment (*SI Appendix*, Figs. S4 *A*–*D* and S5 *A* and *B*). In summary, these findings indicate that sphingolipid synthesis is up-regulated in *Elovl6*$^{-/-}$ BMDMs.

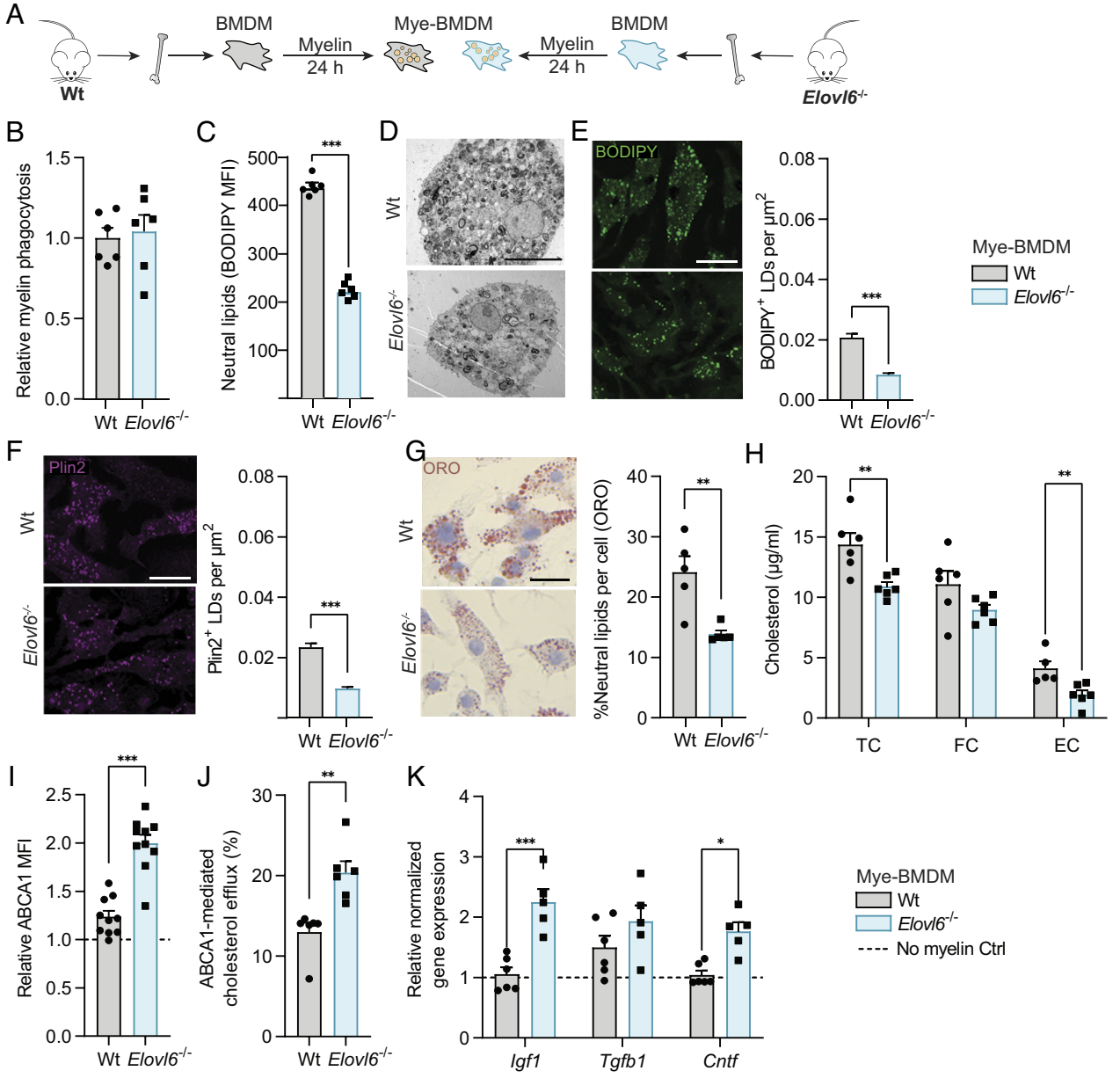

Fig. 2. Elovl6 deficiency promotes intracellular processing of myelin-derived lipids and the induction of a reparative phagocyte phenotype. (*A*) BMDMs were cultured from isolated bone marrow from wild-type (Wt) and *Elovl6* knockout (*Elovl6*$^{-/-}$) mice and stimulated with 24 h of 100 µg/mL myelin. (*B*) Relative fluorescent intensity (MFI) indicating uptake of Dil-labeled myelin by Wt and *Elovl6*$^{-/-}$ BMDMs (N = 6 wells). (*C*) MFI of BODIPY signal measured by FACS in myelin-treated Wt and *Elovl6*$^{-/-}$ BMDMs (N = 6 wells). (*D*) Representative transmission electron microscopy (TEM) image of myelin-treated Wt and *Elovl6*$^{-/-}$ BMDMs showing reduced lipid droplets in *Elovl6*$^{-/-}$ BMDMs. (Scale bar: 10 µm.) (*E*) Representative image of BODIPY-labeled neutral lipids in myelin-treated Wt and *Elovl6*$^{-/-}$ BMDMs, scale bar: 15 µm, and the quantification of the area of BODIPY^{+} lipid droplets per µm^2. (N = 150 to 200 cells from five wells per condition) (*F*) Representative image of IHC staining for Plin2^{+} lipid droplets in myelin-treated Wt and *Elovl6*$^{-/-}$ BMDMs, scale bar: 15 µm, and the quantification of the area of Plin2^{+} lipid droplets per µm^2 (N = 150 to 200 cells from five wells per condition). (*G*) Representative image of ORO staining of myelin-treated Wt and *Elovl6*$^{-/-}$ BMDMs, scale bar: 10 µm, and the quantification of the area of lipids per cell (N = 5 coverslips per genotype). (*H*) Total cholesterol (TC), free cholesterol (FC) and esterified cholesterol (EC) in myelin-treated Wt and *Elovl6*$^{-/-}$ BMDMs (N = 6 wells). (*I*) Flow-cytometric analysis of ABCA1 transporter abundance in myelin-treated BMDMs (N = 10 wells). (*J*) ABCA1 mediated cholesterol efflux in Wt and Elovl6$^{-/-}$ myelin-treated BMDMs (N = 6 wells). (*K*) Gene expression of neurotrophic factors [insulin growth factor 1(*Igf1*), tumor growth factor β (*Tgfb1*), ciliary neurotrophic factor (*Cntf*)] in myelin-treated Wt and Elovl6$^{-/-}$ BMDMs (N = 6 wells) relative to nonmyelin-treated BMDMs. All data are represented as mean ± SEM. **P* < 0.05, ***P* < 0.01, and ****P* < 0.001, Unpaired Student's *t* test.

***Elovl6*$^{-/-}$ Derived FAs Reduce Lipid Load through the S1P/PPARγ Signaling Pathway.** De novo sphingolipid synthesis takes place in the endoplasmic reticulum (ER), where condensation of activated C16 FA palmitoyl-CoA and the amino acid L-serine is catalyzed (18). Since C16 FA levels are increased in *Elovl6*$^{-/-}$ BMDMs, we hypothesized that *Elovl6* deficiency may stimulate de novo sphingolipid synthesis. Therefore, we analyzed the expression of genes involved in sphingolipid synthesis in *Elovl6*$^{-/-}$ macrophages. Indeed, in line with increased levels of DCER and SM, the expression of enzymes involved in their formation, i.e., *Des2*, *Sms1*, *Sms2,* and *Sphk1*, were increased in myelin-treated *Elovl6*$^{-/-}$ BMDMs, with the highest induction of sphingosine kinase 1 (*Sphk1*) (Fig. 3*F* and *SI Appendix*, Fig. S5*C*). SPHK1 catalyzes the phosphorylation of sphingosine to form sphingosine 1-phosphate (S1P) (19), which is one of the most potent bioactive signaling metabolites regulating diverse biological processes (20). By binding to its receptor, S1P receptor 1 (S1PR1), S1P promotes internalization of the receptor (Fig. 3*F* and *SI Appendix*, Fig. S5*D*).

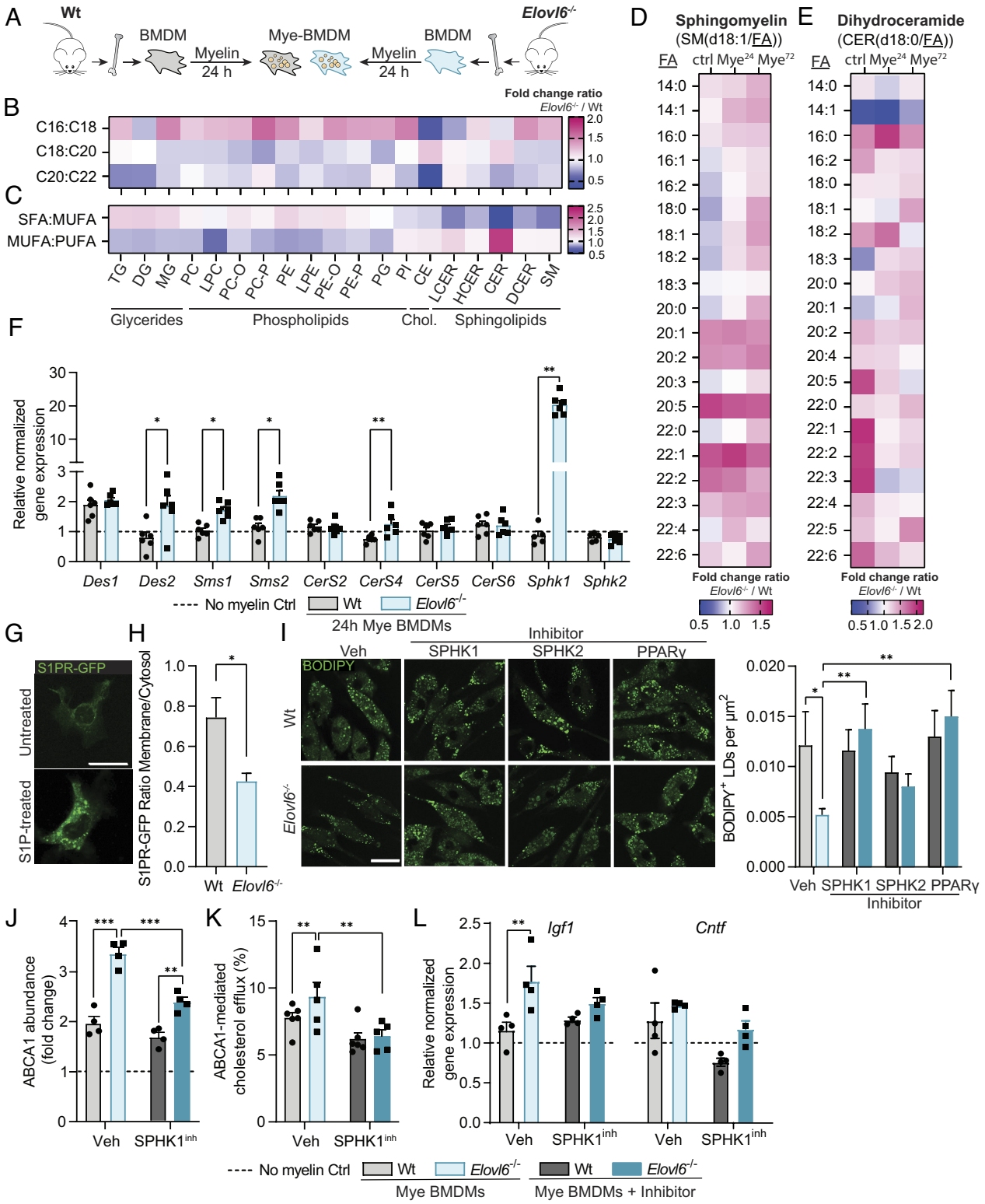

Fig. 3. *Elovl6*$^{-/-}$ derived FAs reduce lipid load through the S1P/PPARγ signaling pathway. (*A*) BMDMs were cultured from isolated bone marrow from wild-type (Wt) and *Elovl6* knockout (*Elovl6*$^{-/-}$) mice and stimulated with 24 h of 100 µg/mL myelin. (*B* and *C*) Ratios of C16:C18, C18:C20, and C20:C22 lipids (*B*) and of saturated (SFA) to monounsaturated fatty acids (MUFAs), and MUFAs to polyunsaturated fatty acis (PUFAs) (*C*) as determined by ESI-MS/MS–based lipidomics in 24-h and 72-h myelin-treated *Elovl6*$^{-/-}$ BMDMs relative to Wt BMDMs (N = 5 wells). LCER=LacCER, HCER=HexCER. (*DE*) Fatty acid composition of sphingomyelin (SM) (*D*) and of dihydroceramides (Cer(d18:0/X), DCER) (*E*) lipid classes in *Elovl6*$^{-/-}$ BMDMs relative to Wt BMDMs (N = 5 wells). (*F*) Gene expression of sphingolipid enzymes of myelin-treated Wt and *Elovl6*$^{-/-}$ BMDMs relative to nonmyelin-treated Ctrl BMDMs (N = 5 wells). (*G*) Representative confocal microscopy images of HEK293 cells stably expressing S1PR1–GFP untreated or treated with S1P. (Scale bar: 20 µm.) (*H*) Quantification of S1PR1-GFP internalization in HEK293 cells stimulated with supernatants from Wt BMDMs and *Elovl6*$^{-/-}$ BMDMs. (N = 35 cells per condition). (*I*) Representative confocal images and quantification of BODIPY^{+} neutral lipids in myelin-treated Wt and *Elovl6*$^{-/-}$ BMDMs treated with SPHK1, SPHK2 and PPARγ inhibitors respectively, scale bar: 20 µm (N = 70 to 85 cells from five wells per condition). (*J*) ABCA1 abundance in myelin-treated Wt and *Elovl6*$^{-/-}$ BMDMS with and without SPHK1 inhibitor (SPHK1^{inh}) relative to no myelin control (N = 4 wells). (*K*) ABCA1 mediated cholesterol efflux in myelin-treated Wt and *Elovl6*$^{-/-}$ BMDMs (N = 5 wells). (*L*) Gene expression of neurotrophic factors (*Igf1*) and (*Cntf*) in myelin-treated Wt and *Elovl6*$^{-/-}$ BMDMs treated with SPHK1 inhibitor (N = 4 wells), relative to no myelin controls. All data are represented as mean ± SEM. **P* < 0.05, ***P* < 0.01 and ****P* < 0.001 Unpaired Student's *t* test (*F*, *H*) and one-way ANOVA (*I*–*L*).

To analyze whether an upregulation of *Sphk1* results in enhanced levels of S1P, we analyzed S1PR1 internalization after incubation with supernatants from Wt and *Elovl6*$^{-/-}$ BMDMs using GFP-labeled S1PR1 (21, 22). Exposure to supernatant of *Elovl6*-deficient BMDMs reduced the S1PR1 membrane to cytosol ratio, indicating increased internalization and thus enhanced levels of S1P excreted by *Elovl6*-deficient BMDMS when compared to Wt BMDMs (Fig. 3*H*). These results confirm increased S1P synthesis in *Elovl6*$^{-/-}$ BMDMs.

The SPHK-S1P signaling axis is an important driver of macrophage metabolism and function, via among others the proliferator-activated receptor gamma (PPARγ) pathway (23). We found that PPARγ-responsive genes, such as *Cd36*, *Lxra,* and *Apoe,* showed significantly increased expression upon *Elovl6*-deficiency (*SI Appendix*, Fig. S5*E*). Therefore, the favorable phenotype of *Elovl6*$^{-/-}$ macrophages may be attributed to enhanced SPHK1 activity and activation of PPARγ. Accordingly, pharmacological inhibition of SPHK1 (PF543), SPHK2 (ABC294640), and PPARγ (GW9662) revealed that SPHK1 and PPARγ, but not SPHK2, underpin the reduced lipid load of *Elovl6*$^{-/-}$ BMDMs (Fig. 3*I*). Accordingly, ABCA1 protein levels, ABCA1-mediated lipid efflux, and *Igf1* expression were reduced in *Elovl6*$^{-/-}$ macrophages treated with the SPHK1 inhibitor (Fig. 3 *J*–*L*). These results point toward SPHK1 being a driver of the metabolic and functional phenotype of *Elovl6*-deficient macrophages.

Lack of Elovl6 Stimulates Remyelination in an Ex Vivo Cerebellar Brain Slice (BSC) Model. In MS, progressive axonal degeneration and permanent disability are driven by demyelination and failure of remyelination (24). Increasing evidence indicates that macrophages and microglia promote remyelination by producing neurotrophic factors (25), and that metabolic dysfunction due to lipid overload counteracts these reparative features (10). Since our in vitro data indicate that *Elovl6* deficiency increases the expression of neurotrophic factors and improves the metabolism of myelin-derived lipids, we next determined the impact of *Elovl6* deficiency on demyelination and myelin repair using organotypic cerebellar brain slices (BSCs) demyelinated with lysolecithin (Fig. 4*A*). In agreement with our in vitro findings, absence of *Elovl6* reduced the intracellular LDs load in macrophages and microglia in BSCs (Fig. 4*B* and *SI Appendix*, Fig. S6*A*). In addition, fluorescent staining demonstrated increased colocalization of myelin basic protein (MBP) with axons (neurofilament, NF) in *Elovl6*$^{-/-}$ BSCs directly after lysolecithin treatment (*SI Appendix*, Fig. S6 *B* and *C*) and after 1 wk of remyelination (Fig. 4 *C* and *D*). Three-dimensional reconstruction of these sections confirmed that there is more axonal myelination in *Elovl6*$^{-/-}$ slices. Paranodal length and density, measured by quantifying Caspr^{+} paranodes in Wt and *Elovl6*$^{-/-}$ slices, did not significantly differ (*SI Appendix*, Fig. S6 *D*–*F*). All in all, these findings indicate that *Elovl6* deficiency protects against lysolecithin-induced demyelination and enhances efficient remyelination. Consistent with these findings, BSCs showed an elevated expression of *Pdgfa*, *Plp,* and *Mog* and increased abundance of OLIG2^{+}CC1^{+} mature oligodendrocytes (Fig. 4*D* and *SI Appendix*, Fig. S6 *C* and *E*). In contrast to our in vitro findings, *Elovl6* deficiency did not increase the expression

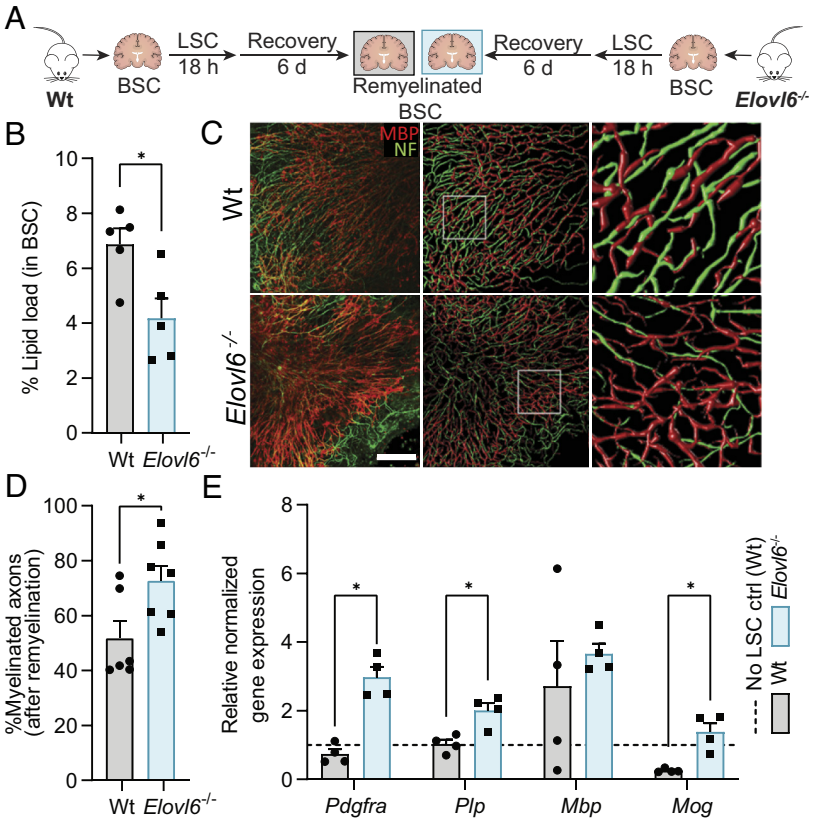

Fig. 4. *Elovl6* deficiency stimulates remyelination in ex vivo brain slice cultures (BSC). (*A*) Brain slices were isolated from p10 Wt and *Elovl6*$^{-/-}$ mouse pups, demyelinated with lisolecithin (LSC) for 18 h and recovered in basal medium for 6 d after which remyelination was assessed. (*B*) Percentage area of lipid droplets in total brain slice area as determined by ORO staining (N = 5 slices). (*C*) Representative immunofluorescence images of remyelinated BSC (d6) stained for myelin basic protein (MBP) and neurofilament (NF) (Wt N = 6 and *Elovl6*$^{-/-}$ N = 7 slices) (Scale bar: 50 µm; orthogonal and three-dimensional reconstruction). (*D*) Percentage of MBP^{+}NF^{+} axons out of total NF^{+} axons in Wt and *Elovl6*$^{-/-}$ BSCs (N = 7 slices). (*E*) Gene expression of oligodendrocyte maturation markers [platelet-derived growth factor receptor α (*Pdgfra*), myelin proteolipid protein (*Plp*), myelin basic protein (*Mbp*), myelin oligodendrocyte glycoprotein (*Mog*)] after remyelination relative to no-LSC-treated control. All data are represented as mean ± SEM. **P* < 0.05, ***P* < 0.01, and ****P* < 0.001, one-way ANOVA.

of neurotrophic factors in ex vivo BSC (*SI Appendix*, Fig. S6*F*), while it did decrease the expression of inflammatory mediators such as *Ccl4* (*SI Appendix*, Fig. S6*G*). Collectively, these findings show that *Elovl6* deficiency reduces phagocyte lipid load, protects against demyelination, and enhances remyelination.

***Elovl6* Deficiency Stimulates Remyelination In Vivo.** To validate the reparative impact of *Elovl6*$^{-/-}$ in vivo, the mouse cuprizone model was used in which prominent demyelination occurs in different areas of the CNS, in particular in the corpus callosum (26). Mice were fed with 0.3% cuprizone for 6 wk, followed by 1 wk of normal diet during which remyelination occurs. Curpizone-fed mice were pathologically characterized after demyelination (6 wk) and during spontaneous remyelination (6 wk + 1) (Fig. 5*A*). MBP staining and g-ratio analysis showed more myelination after cuprizone-induced demyelination (6 wk) and after spontaneous remyelination (6 wk + 1) in *Elovl6*$^{-/-}$ compared to Wt mice (Fig. 5 *B*–*F*). Similar to our in vitro experiments, an increased expression of neurotrophic factors *Tgf1b* and *Cntf* was found in the corpus callosum of *Elovl6*$^{-/-}$ mice after demyelination, and of *Igf1* after both demyelination and remyelination (Fig. 5*G* and *SI Appendix*, Fig. S7*A*). Moreover, a reduction of inflammatory mediators was observed after both demyelination (6 wk) and remyelination (6 wk + 1) (Fig. 5*H*, *SI Appendix*, Fig. S7*B*). These findings demonstrate that *Elovl6* deficiency protects against demyelination and promotes remyelination in the cuprizone-induced demyelination model.

To determine the impact of *Elovl6*$^{-/-}$ on lipid metabolism in vivo, we first assessed foam cell formation after demyelination. ORO staining showed a significant reduction of cellular lipid load after demyelination and during remyelination in the corpus callosum of cuprizone-fed *Elovl6*$^{-/-}$ mice (*SI Appendix*, Fig. S7 *C* and *D*). This reduction in lipid load coincided with increased protein abundance of ABCA1 during demyelination (*SI Appendix*, Fig. S7 *E*–*G*). Accordingly, lipidomic analysis demonstrated reduced levels of cholesterol esters in the corpus callosum of *Elovl6*$^{-/-}$ mice (*SI Appendix*, Fig. S7*J*). Notably, *Elovl6*$^{-/-}$ mice had a significantly lower abundance of F4/80^{+} phagocytes during demyelination (*SI Appendix*, Fig. S7 *E* and *H*). In line with our in vitro data, lipidomics enrichment analysis showed an increase in C16 FAs, specifically C16:0 (*SI Appendix*, Fig. S8 *A* and *B*) in the corpus callosum of *Elovl6*$^{-/-}$ mice, indicating reduced elongation of C16 FAs. Finally, gene expression analysis showed increased expression of *Sphk1* in the corpus callosum (*SI Appendix*, Fig. S7*I*). All in all, these findings suggest that internalized myelin is more efficiently processed and effluxed in phagocytes in *Elovl6*$^{-/-}$ mice during demyelination in vivo.

Phagocyte-Specific *Elovl6* Deficiency Stimulates Remyelination In Vivo. To determine whether the observed effects of *Elovl6*$^{-/-}$ mice can be attributed to macrophages and microglia specifically, we generated phagocyte-specific *Elovl6*$^{-/-}$ mice and induced cuprizone-mediated demyelination. Depletion of *Elovl6* in macrophages and microglia was achieved by crossing *Elovl6*$^{fl+/+}$ mice with *LysMCre*$^{+/-}$ mice (Fig. 6*A*). *Elovl6* ablation in phagocytes was validated by quantitative gene expression (*SI Appendix*, Fig. S9 *A* and *B*). In contrast to full *Elovl6* knockout, *Elovl6*$^{fl/fl}$*LysMCre*$^{+/-}$ mice displayed no differences in MBP area after the demyelination phase (6 wk) (Fig. 6 *B* and *D*). However, phagocyte-specific *Elovl6* knockout did show increased MBP reactivity during remyelination (6 wk + 1; Fig. 6 *B* and *D*) in line with full *Elovl6* knockout. Consistent with enhanced remyelination, *Elovl6*$^{fl+/+}$*LysMCre*$^{+/-}$ mice showed decreased lipid load and increased ABCA1 abundance within phagocytes during remyelination, but not after demyelination (Fig. 6 *E*–*G*). *Elovl6*$^{fl+/+}$*LysMCre*$^{+/-}$ mice also demonstrated an increased expression of neurotrophic factors (*Igf1* and *Cntf*) (Fig. 6 *H* and *I*). These data confirm that *Elovl6* deficiency enhances remyelination, at least in part, by promoting the reparative properties of phagocytes.

Discussion

Increasing evidence indicates that impaired metabolic processing of myelin-derived lipids skews macrophages and microglia towards a disease-promoting phenotype in demyelinating disorders (10, 11, 15, 27). Here, we show that ELOVL6 is a key enzyme in the induction of this lesion-promoting phagocyte phenotype during demyelination. Genetic deficiency of Elovl6 showed several beneficial effects in animal models of demyelinating disorders, including reduced intracellular lipid accumulation, increased expressed neurotrophic factor genes, and improved remyelination. These findings suggest that inhibiting ELOVL6 may be a promising therapeutic approach for demyelinating disorders (Fig. 7).

In MS, axonal degeneration and permanent disability are driven by demyelination with progressive failure of remyelination (24). Although endogenous remyelination occurs, it is often incomplete and fails over time (28). Several studies have indicated that phagocytes drive remyelination by producing neurotrophic factors such as IGF-1, TGF-β, and CNTF (5, 25, 29). These neurotrophic factors enhance oligodendrocyte survival and support differentiation by increasing cell ramification and production of myelin proteins (30). In demyelinating disorders, foamy phagocytes accumulate a large number of cytosolic lipid droplets containing an inert storage pool of neutral lipids of which the major component is cholesterol (31). We show that *Elovl6*$^{-/-}$ BMDMs treated with myelin showed a reduction in lipid storage and cholesterol levels, which was accompanied by an increase in ABCA1 protein abundance and lipid efflux. This is consistent with a previous study where *Elovl6* depletion markedly reduced lipid load in foamy macrophages in atherosclerosis by enhancing the expression of ABCA1 (32). This strongly suggests that modifying fatty acid elongation can impact the metabolic properties of myelin-laden phagocytes in an ABCA1-dependent manner (Fig. 7). Our findings suggest that the absence of *Elovl6* prevents lysolecithin and cuprizone-induced demyelination and provides a permissive environment for remyelination by reducing foam cell formation and enhancing the expression of neuroprotective factors.

While global *Elovl6* knockout mice displayed reduced phagocyte lipid load only directly after demyelination, phagocyte-specific *Elovl6* knockout mice showed increased myelination and a reduced lipid load during remyelination and not after demyelination. Phagocyte-specific *Elovl6* deficiency also resulted in increased expression of neurotrophic factors in the CNS, but the induction was not as pronounced compared to the full knockout, suggesting that *Elovl6* deficiency controls the regenerative properties of other cell types as well. For instance, as *Elovl6* was found to be expressed in oligodendrocytes as well, deficiency of the enzyme in these myelin-producing glial cells, may impact their proliferation and/or differentiation. Of note, our data indicate an upregulation of genes linked to oligodendrocyte differentiation and remyelination in the *Elovl6*$^{-/-}$ BSCs, in particular *Pdgfra*. PDGFα-PDGFRα signaling stimulates OPC proliferation following demyelination and acts as an important survival factor during remyelination (33), consistent with the increased number of OPCs observed in our *Elovl6*$^{-/-}$ BSCs. Moreover, previous studies have reported that overexpression or treatment with PDGFα promotes remyelination in vivo (34). Another possibility would be a direct impact of ELOVL6 in astrocytic FA synthesis, essential for neuronal differentiation during

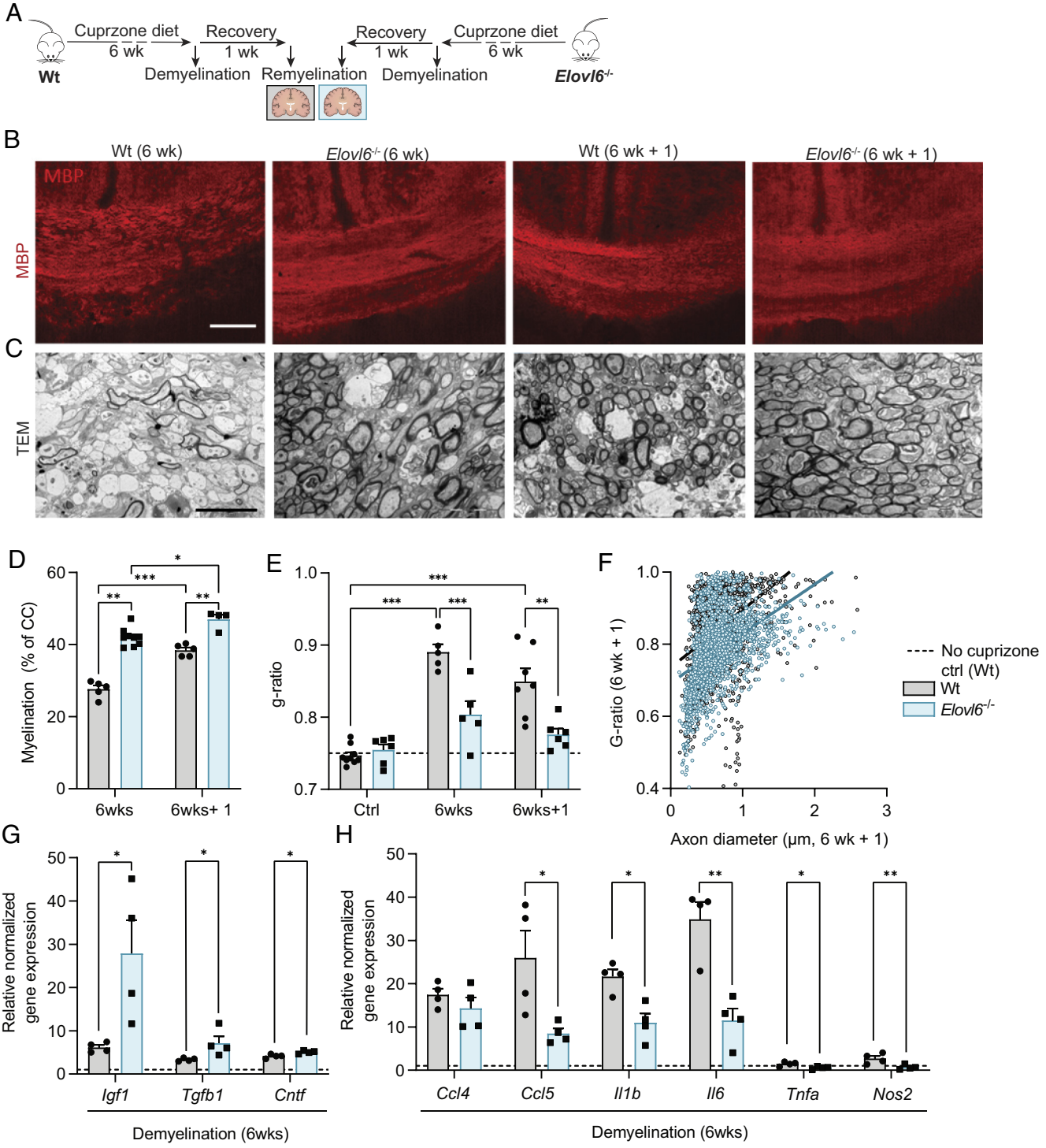

Fig. 5. *Elovl6* deficiency stimulates remyelination after in vivo cuprizone-induced demyelination. (*A*) Wt and *Elovl6*$^{-/-}$ mice received a cuprizone diet to induce demyelination for 6 wk, followed up by a 1-wk recovery period (6 wk + 1) on a normal diet after which brains were collected for further analyses. (*B* and *C*) Representative images of MBP staining (*B*) and TEM (*C*) of the corpus callosum (CC) from Wt and *Elovl6*$^{-/-}$after 6 wk and 6 wk + 1, scale bar: 100 µm MBP; 5 µm TEM. (*D*) Percentage of MBP+ area in the CC of Wt and *Elovl6*$^{-/-}$ mice [N = 4 (6 wk), N = 5 (6 wk + 1)]. (*E* and *F*) Analysis of the g-ratio (the ratio of the inner axonal diameter to the total outer diameter) (*E*) and as a function of axon diameter in CC (*F*) from Wt [Ctrl (no cuprizone), N = 6; 6 wk, N = 3 animals; 6 wk + 1, N = 4 animals] and *Elovl6*$^{-/-}$ mice [Ctrl (no cuprizone), N = 6; 6 wk, N = 4 animals; 6 wk + 1, N = 3 animals]. (*G* and *I*) Gene expression of neurotrophic factors (*G*) and inflammatory genes (*H*) in the corpus callosum (CC) of Wt and *Elovl6*$^{-/-}$ mice after cuprizone treatment (6 wk, N = 4 animals) relative to no cuprizone controls. All data are represented as mean ± SEM. **P* < 0.05, ***P* < 0.01, and ****P* < 0.001, one-way ANOVA.

development (35). However, we could not observe ELOVL6 protein in GFAP^{+} astrocytes in MS lesions, and this is therefore more unlikely. Further research should be conducted to unravel the role of ELOVL6 in other CNS cell types.

Consistent with previous studies (36, 37), reduced ELOVL6 activity alters the FA profile of phagocytes by increasing the amount of palmitic acid (C16:0) and palmitoleic acid (C16:1) (38–40). Palmitic acid is the precursor of palmitoyl-CoA, the primary molecule in de novo sphingolipid synthesis. Our data show an upregulation of genes involved in sphingolipid synthesis in *Elovl6*-deficient macrophages, in particular *Sphk1*. SPHK presents two isoforms, SPHK1 and SPHK2, which have opposing roles in the regulation

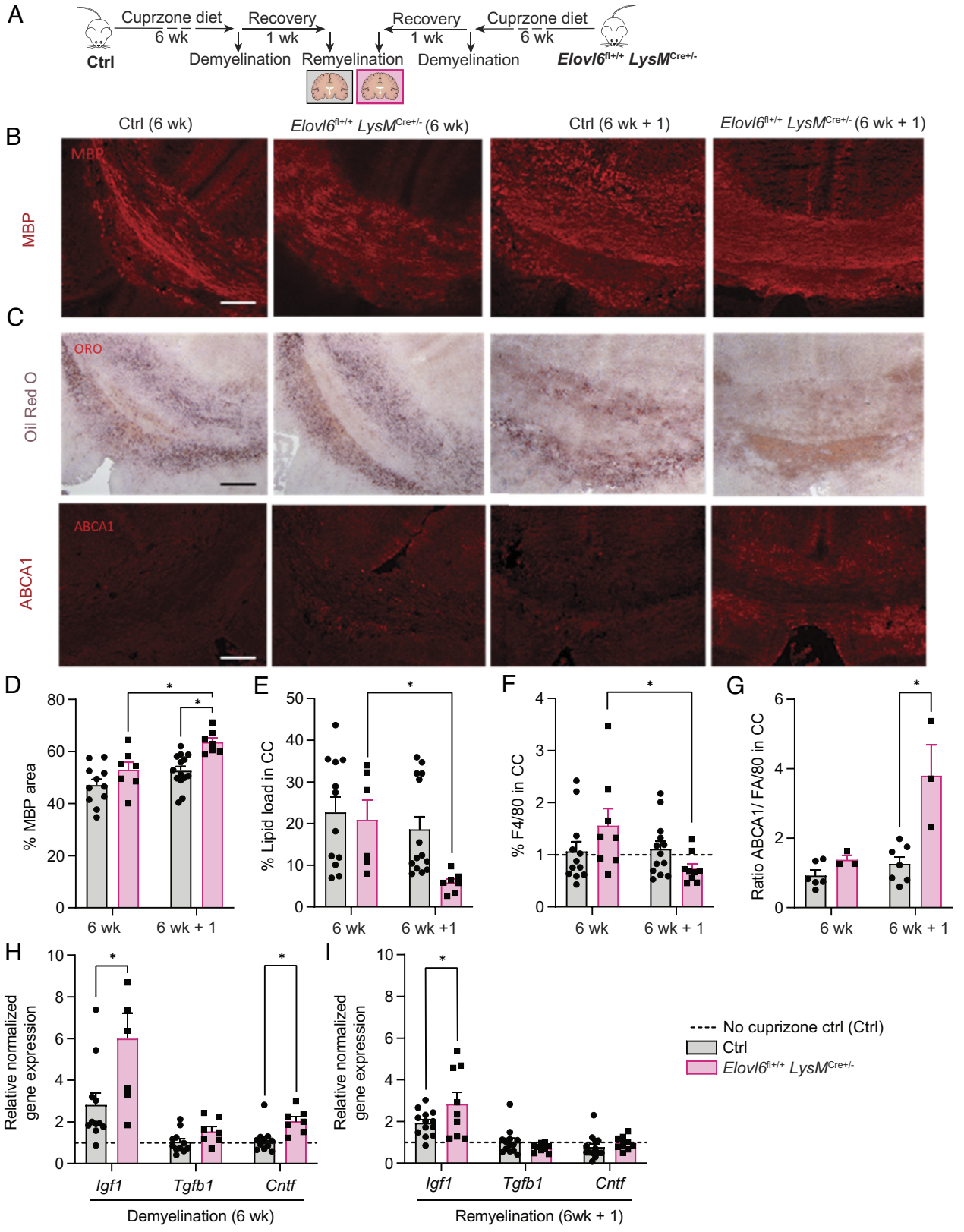

Fig. 6. Phagocyte-specific *Elovl6* deficiency stimulates remyelination in vivo. (*A*) Control (Ctrl; *Elovl6*$^{fl+/+}$*LysMcre*$^{-/-}$) and phagocyte-specific *Elovl6*$^{-/-}$ mice (*Elovl6*$^{fl+/+}$*LysMcre*$^{+/-}$) received a cuprizone diet for 6 wk to induce demyelination, followed up by a 1-wk recovery period (6 wk + 1) on a normal diet after which brains were collected for further analyses. (*B* and *C*) Representative images of immunofluorescent MBP staining (*B*) and of ORO and immunofluorescent ABCA1 staining (*C*) of corpus callosum (CC) from control mice and *Elovl6*$^{fl+/+}$*LysMcre*$^{+/-}$ mice after 6 wk and 6 wk + 1. (Scale bar: 100 µm.) (Ctrl, N = 10 animals; *Elovl6*$^{fl+/+}$*LysMcre*$^{+/-}$, N = 6 animals). (*D*) Quantitative analysis of MBP-positive area in the CC from Ctrl (N = 10 animals) and *Elovl6*$^{fl+/+}$*LysMcre*$^{+/-}$ animals (N = 3 to 6). (*E*) Percentage lipid load as ORO^{+} area of the total CC area. (*F*) Percentage of F4/80^{+} in total CC area of Ctrl and *Elovl6*$^{fl+/+}$*LysMcre*$^{+/-}$ animals. (*G*) Percentage of ABCA1^{+} area of total CC area corrected for the percentage of F4/80^{+} in the CC from Ctrl and *Elovl6*$^{fl+/+}$*LysMcre*$^{+/-}$ animals. (*H* and *I*) Gene expression of neurotrophic factors in the CC from Ctrl (N = 10 animals) and *Elovl6*$^{fl+/+}$*LysMcre*$^{+/-}$ (N = 6 to 7 animals) mice after 6 wk (*H*) and 6 wk + 1 (*I*) relative to no-cuprizone controls. All data are represented as mean ± SEM. *P < 0.05, **P < 0.01, and ***P < 0.001, one-way ANOVA.

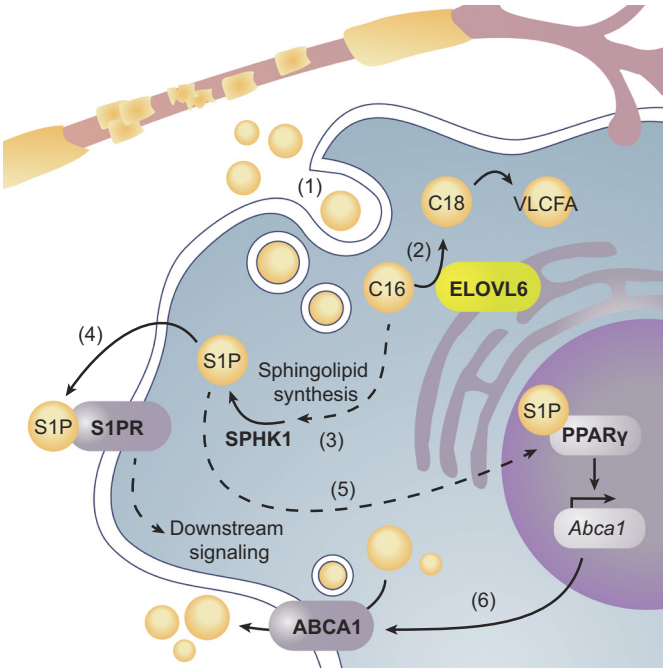

Fig. 7. ELOVL6 deficiency alters lipid metabolism in myelin-phagocytosing macrophages (1) Excessive myelin uptake results in lipid-loaded macrophages with enhanced ELOVL6 activation. (2) ELOVL6 activity decreases C16/C18 ratios and increases very long-chain fatty acid (VLCFA) levels. (3) *Elovl6*$^{-/-}$ increases levels of C16 FAs, which feed sphingolipid synthesis and enhance the production of spingosine-1-phosphate (S1P) via increasing *Sphk1* expression. (4) Interaction of S1P with its receptor S1PR results in further downstream signaling via among others Akt. (5) Additionally, S1P can interact with the nuclear receptor PPARγ that can induce the expression of *Abca1*. (6) Increased levels of ABCA1 mediate enhanced lipid efflux resulting in lowers lipid load in *Elovl6*-deficient macrophages

of ceramide biosynthesis and suggest that the intracellular location of S1P production dictates its functions (19). SPHK1 is located mainly in the cell membrane, cytoplasm, and lysosomes, while SPHK2 is mainly located in the nucleus, ER, and mitochondria (19, 41). Our data show that *Elovl6* deficiency increases the production of S1P via SPHK1 upregulation. S1P is an important regulator of cellular lipid metabolism, and its endogenous generation and signaling were recently identified as a major regulator of ABCA1-mediated cholesterol efflux in macrophages (42, 43). Our data show that the suppression of the de novo S1P production by SPHK1 inhibition reduces ABCA1 protein abundance and, consequently, decreases lipid efflux. In addition, S1P has been linked to the polarization of macrophages, although contradictory findings are reported (20). Our data also showed that SPHK1 inhibition reverted the induction of *Igf1* by *Elovl6* deficiency. A study by Weigert et al. showed that intracellular S1P produced by SPHK1 generally promotes inflammatory macrophage activity (21). In contrast, Parket al. reported that S1P also induces M2 polarization of macrophages via IL-4 signaling (44). In accordance with the latter, our findings suggest that increased production of S1P in *Elovl6*-deficient cells may polarize them toward a reparative phenotype. Interestingly, S1P signaling was recently reported to promote neuroinflammation (45). While inhibition of S1P was associated with reduced disease progression of the mouse neuroinflammatory MS model, experimental autoimmune encephalitis (EAE), our data rather presents a positive effect in a remyelination model of MS. This highlights the pleiotropic roles S1P can play during inflammatory and reparative phases of disease.

Our findings indicate that the activation or the S1P/PPARγ axis underlies the repair-promoting macrophage phenotype observed in *Elovl6*-deficient macrophages. We show that PPARγ activity is enhanced in *Elovl6*$^{-/-}$ macrophages upon myelin exposure, and that the observed reduced lipid load and ABCA1 abundance are controlled by PPARγ in these cells. S1P is a direct ligand of PPARγ, and endogenous S1P production elevates PPARγ protein expression (23). PPARγ activation inhibits innate immune cell activation and foam cell formation and promotes macrophage polarization to an anti-inflammatory phenotype by reducing the production of proinflammatory cytokines such as TNFα and IL-6 (7, 46–48). In line with these findings, we demonstrated in one of our previous studies that myelin-treated macrophages display a marked increase in LDs when PPARγ activity is suppressed (49). Next to the activation of PPARs, S1P can also activate PI3K/Akt signaling. This pathway regulates macrophage survival, migration, and proliferation and coordinates their response to different inflammatory and metabolic signals (50). A recent study shows that *Elovl6* deficiency leads to an induction of the PI3K/Akt pathway (36), which, based on our findings, may be mediated by S1P. During the last decades, there has been an increasing interest in S1PR modulators for the treatment of MS. Modulators such as fingolimod and siponimod have been approved for the treatment of RRMS and progressive MS patients due to their efficacy in managing neurodegenerative aspects of the disease (51, 52). Our findings indicate that block of *Elovl6* activity during demyelination enhances endogenous S1P synthesis which limits demyelination and enhances CNS repair.

In addition, other fatty acid species, like palmitoleic and oleic acid, that we found to be elevated after ELOVL6 depletion may contribute to the observed effects. Palmitoleic acid and oleic acid are known for their anti-inflammatory properties (39, 40). Palmitoleic acid has been shown to protect BMDMs against the proinflammatory effects of SFAs by increasing the phosphorylation of AMPK (53). In several studies, oleic acid was found to have anti-inflammatory properties, facilitating the polarization of phagocytes to a wound-healing phenotype (39, 54). Finally, the effects induced by *Elovl6* deficiency effect may be driven by the reduction of ratios of very long-chain fatty acids (VLCFA) to LCFAs. ELOVL6 catalyzes the elongation of FA with 12, 14, and 16 carbons, playing a key role in de novo synthesis of VLCFAs by preceding the rest of ELOVLs in the elongation process by generating precursors (13, 14). These VLCFA are elevated in MS patients and are associated with the induction of inflammation and neurodegeneration in the brain (55).

In summary, this study demonstrates that targeting FA elongation by inhibiting ELOVL6 is a promising strategy to promote remyelination in demyelinating diseases such as MS and other neurodegenerative diseases.

Materials and Methods

BMDMs were primarily cultured from female Wt C57BL/6J mice purchased from Envigo. *Elovl6* Knockout mice (*Elovl6*$^{-/-}$ mice, C57BL/6 background) were kindly provided by prof. dr. Takashi Matsuzaka (Department of Endocrinology and Metabolism, University of Tsukuba, Japan) and bred in our facility. To generate phagocyte-specific *Elovl6*$^{-/-}$ mice, *Elovl6*$^{fl+/+}$ mice were intercrossed with C57BL/6J *LysMCre* mice, which were also kindly provided by Takashi Matsuzaka (Department of Endocrinology and Metabolism, University of Tsukuba, Japan). Mice were housed in the animal facility of the Biomedical Research Institute of Hasselt University and kept in a daily cycle of 12-h light and 12-h darkness (LD 12:12) with free access to water and a standard chow diet. All experiments were conducted in accordance with the institutional guidelines and approved by the Ethical Committee for Animal Experiments of Hasselt University. The detailed methods for cell culture, lipidomics, phagocytosis analysis, cholesterol measurements, flow cytometry, S1PR-GFP internalization assay, immunostaining, PCR, cuprizone model, histological analysis, and statistical analysis can be found in *SI Appendix, Materials and Methods*.

Data, Materials, and Software Availability. All study data reported in the article and/or *SI Appendix* will be shared by the lead contact upon request. This paper does not report original code nor generate new unique reagents. Any additional information required to reanalyze the data reported in this paper is available from the lead contact upon request.

ACKNOWLEDGMENTS. We thank M.P. Tulleners and Frank Vanderhoydonc for their excellent technical assistance. We also thank Susan Schwab and her team (Skirball Institute of Biomolecular Medicine, New York University Langone Medical Center, USA) for providing the S1PR-GFP plasmids. The work was financially supported by the Research Foundation of Flanders (FWO Vlaanderen; G099618FWO and SBO-LipoMacs-S001623N), the Interreg V-A EMR program (EURLIPIDS and EMR23), the Belgian Charcot Foundation (2019-0009), and the special research fund UHasselt (BOF). The funding agencies had no role in the design, analysis, or writing of the article.

Author affiliations: [a]Department of Immunology and Infection, Biomedical Research Institute, Hasselt University, Diepenbeek 3590, Belgium; [b]Department of Oncology, Laboratory of Lipid Metabolism and Cancer, Leuven Cancer Institute, University of Leuven, Leuven 3000, Belgium; [c]Department of Cardiology and Organ Systems, Biomedical Research Institute, Hasselt University, Diepenbeek 3590, Belgium; and [d]Department of Internal Medicine (Endocrinology and Metabolism), Faculty of Medicine, University of Tsukuba, Tsukuba, Ibaraki 305-8575, Japan

Author contributions: A.V.G.C., S.G.S.V., M.H., T.W., J.F.J.B., and J.J.A.H. designed research; A.V.G.C., S.G.S.V., E.G., S.V., M.L., T.W., P.G., I.L., J.F.J.B., and J.J.A.H. performed research; M.H., J.D., P.G., T.M., I.L., and J.V.S. contributed new reagents/analytic tools; A.V.G.C., S.G.S.V., M.H., J.D., T.W., and J.F.J.B. analyzed data; and A.V.G.C., S.G.S.V., M.H., J.F.J.B., and J.J.A.H. wrote the paper.

1. N. Koch-Henriksen, P. S. Sorensen, The changing demographic pattern of multiple sclerosis epidemiology. *Lancet Neurol.* **9**, 520–532 (2010).
2. J. F. Bogie, P. Stinissen, J. J. Hendriks, Macrophage subsets and microglia in multiple sclerosis. *Acta Neuropathol.* **128**, 191–213 (2014).
3. J. W. Prineas, J. D. E. Parratt, Multiple sclerosis: Microglia, monocytes, and macrophage-mediated demyelination. *J. Neuropathol. Exp. Neurol.* **80**, 975–996 (2021).
4. D. Y. Vogel *et al.*, Macrophages in inflammatory multiple sclerosis lesions have an intermediate activation status. *J. Neuroinflammation* **10**, 35 (2013).
5. V. E. Miron *et al.*, M2 microglia and macrophages drive oligodendrocyte differentiation during CNS remyelination. *Nat. Neurosci.* **16**, 1211–1218 (2013).
6. J. M. Ruckh *et al.*, Rejuvenation of regeneration in the aging central nervous system. *Cell Stem Cell* **10**, 96–103 (2012).
7. J. F. Bogie *et al.*, Myelin alters the inflammatory phenotype of macrophages by activating PPARs. *Acta Neuropathol. Commun.* **1**, 43 (2013).
8. J. F. Bogie *et al.*, Myelin-derived lipids modulate macrophage activity by liver X receptor activation. *PLoS One* **7**, e44998 (2012).
9. L. A. Boven *et al.*, Myelin-laden macrophages are anti-inflammatory, consistent with foam cells in multiple sclerosis. *Brain* **129**, 517–526 (2006).
10. J. F. J. Bogie *et al.*, Stearoyl-CoA desaturase-1 impairs the reparative properties of macrophages and microglia in the brain. *J. Exp. Med.* **217**, e20191660 (2020).
11. J. F. J. Bogie, M. Haidar, G. Kooij, J. J. A. Hendriks, Fatty acid metabolism in the progression and resolution of CNS disorders. *Adv. Drug. Deliv. Rev.* **159**, 198–213 (2020).
12. A. V. Garcia Corrales, M. Haidar, J. F. J. Bogie, J. J. A. Hendriks, Fatty acid synthesis in glial cells of the CNS. *Int. J. Mol. Sci.* **22**, 8159 (2021).
13. H. Guillou, D. Zadravec, P. G. Martin, A. Jacobsson, The key roles of elongases and desaturases in mammalian fatty acid metabolism: Insights from transgenic mice. *Prog. Lipid. Res.* **49**, 186–199 (2010).
14. D. B. Jump, Mammalian fatty acid elongases. *Methods Mol. Biol.* **579**, 375–389 (2009).
15. L. Cantuti-Castelvetri *et al.*, Defective cholesterol clearance limits remyelination in the aged central nervous system. *Science* **359**, 684–688 (2018).
16. J. Marschallinger *et al.*, Lipid-droplet-accumulating microglia represent a dysfunctional and proinflammatory state in the aging brain. *Nat. Neurosci.* **23**, 194–208 (2020).
17. M. R. Molenaar *et al.*, LION/web: A web-based ontology enrichment tool for lipidomic data analysis. *Gigascience* **8**, giz061 (2019).
18. D. Wigger, E. Gulbins, B. Kleuser, F. Schumacher, Monitoring the sphingolipid de novo synthesis by stable-isotope labeling and liquid chromatography-mass spectrometry. *Front Cell Dev. Biol.* **7**, 210 (2019).
19. M. Maceyka *et al.*, SphK1 and SphK2, sphingosine kinase isoenzymes with opposing functions in sphingolipid metabolism. *J. Biol. Chem.* **280**, 37118–37129 (2005).
20. A. Weigert, C. Olesch, B. Brune, Sphingosine-1-phosphate and macrophage biology-how the sphinx tames the big eater. *Front Immunol.* **10**, 1706 (2019).
21. A. Baeyens *et al.*, Monocyte-derived S1P in the lymph node regulates immune responses. *Nature* **592**, 290–295 (2021).
22. A. A. L. Baeyens, S. R. Schwab, Finding a way out: S1P signaling and immune cell migration. *Annu. Rev. Immunol.* **38**, 759–784 (2020).
23. K. A. Parham *et al.*, Sphingosine 1-phosphate is a ligand for peroxisome proliferator-activated receptor-gamma that regulates neoangiogenesis. *FASEB J.* **29**, 3638–3653 (2015).
24. J. Correale, M. Marrodan, M. C. Ysrraelit, Mechanisms of neurodegeneration and axonal dysfunction in progressive multiple sclerosis. *Biomedicines* **7**, 14 (2019).
25. K. S. Rawji, M. K. Mishra, V. W. Yong, Regenerative capacity of macrophages for remyelination. *Front Cell Dev. Biol.* **4**, 47 (2016).
26. G. K. Matsushima, P. Morell, The neurotoxicant, cuprizone, as a model to study demyelination and remyelination in the central nervous system. *Brain Pathol.* **11**, 107–116 (2001).
27. H. Yu, S. Bai, Y. Hao, Y. Guan, Fatty acids role in multiple sclerosis as "metabokines". *J. Neuroinflammation* **19**, 157 (2022).
28. R. J. Franklin, C. Ffrench-Constant, Remyelination in the CNS: From biology to therapy. *Nat. Rev. Neurosci.* **9**, 839–855 (2008).
29. M. R. Kotter, C. Zhao, N. van Rooijen, R. J. Franklin, Macrophage-depletion induced impairment of experimental CNS remyelination is associated with a reduced oligodendrocyte progenitor cell response and altered growth factor expression. *Neurobiol. Dis.* **18**, 166–175 (2005).
30. J. Zhang *et al.*, Targeting oligodendrocyte protection and remyelination in multiple sclerosis. *Mt Sinai J. Med.* **78**, 244–257 (2011).
31. T. Y. Chang, C. C. Chang, N. Ohgami, Y. Yamauchi, Cholesterol sensing, trafficking, and esterification. *Annu. Rev. Cell Dev. Biol.* **22**, 129–157 (2006).
32. R. Saito *et al.*, Macrophage Elovl6 deficiency ameliorates foam cell formation and reduces atherosclerosis in low-density lipoprotein receptor-deficient mice. *Arterioscler Thromb Vasc Biol.* **31**, 1973–1979 (2011).
33. R. C. Armstrong, Growth factor regulation of remyelination: Behind the growing interest in endogenous cell repair of the CNS. *Future Neurol.* **2**, 689–697 (2007).
34. A. C. Vana *et al.*, Platelet-derived growth factor promotes repair of chronically demyelinated white matter. *J. Neuropathol. Exp. Neurol.* **66**, 975–988 (2007).
35. A. Tabernero, E. M. Lavado, B. Granda, A. Velasco, J. M. Medina, Neuronal differentiation is triggered by oleic acid synthesized and released by astrocytes. *J. Neurochem.* **79**, 606–616 (2001).
36. T. Matsuzaka *et al.*, Hepatocyte ELOVL fatty acid Elongase 6 determines ceramide acyl-chain length and hepatic insulin sensitivity in mice. *Hepatology* **71**, 1609–1625 (2020).
37. T. Matsuzaka *et al.*, Crucial role of a long-chain fatty acid elongase, Elovl6, in obesity-induced insulin resistance. *Nat. Med.* **13**, 1193–1202 (2007).
38. H. Shimano, Novel qualitative aspects of tissue fatty acids related to metabolic regulation: Lessons from Elovl6 knockout. *Prog. Lipid. Res.* **51**, 267–271 (2012).
39. C. Carrillo, M. Cavia Mdel, S. Alonso-Torre, Role of oleic acid in immune system; mechanism of action; a review. *Nutr. Hosp.* **27**, 978–990 (2012).
40. C. O. Souza *et al.*, Palmitoleic acid reduces the inflammation in LPS-stimulated macrophages by inhibition of NFkappaB, independently of PPARs. *Clin. Exp. Pharmacol. Physiol.* **44**, 566–575 (2017).
41. D. Hatoum, N. Haddadi, Y. Lin, N. T. Nassif, E. M. McGowan, Mammalian sphingosine kinase (SphK) isoenzymes and isoform expression: Challenges for SphK as an oncotarget. *Oncotarget* **8**, 36898–36929 (2017).
42. S. Spiegel, S. Milstien, The outs and the ins of sphingosine-1-phosphate in immunity. *Nat. Rev. Immunol.* **11**, 403–415 (2011).
43. M. Vaidya *et al.*, Regulation of ABCA1-mediated cholesterol efflux by sphingosine-1-phosphate signaling in macrophages. *J. Lipid. Res.* **60**, 506–515 (2019).
44. S. J. Park *et al.*, Sphingosine 1-phosphate induced anti-atherogenic and atheroprotective M2 macrophage polarization through IL-4. *Cell Signal* **26**, 2249–2258 (2014).
45. H. L. Chung *et al.*, Very-long-chain fatty acids induce glial-derived sphingosine-1-phosphate synthesis, secretion, and neuroinflammation. *Cell Metab.* **35**, 855–874.e855 (2023).
46. M. Ricote, A. F. Valledor, C. K. Glass, Decoding transcriptional programs regulated by PPARs and LXRs in the macrophage: Effects on lipid homeostasis, inflammation, and atherosclerosis. *Arterioscler. Thromb. Vasc. Biol.* **24**, 230–239 (2004).
47. E. Rigamonti, G. Chinetti-Gbaguidi, B. Staels, Regulation of macrophage functions by PPAR-alpha, PPAR-gamma, and LXRs in mice and men. *Arterioscler. Thromb. Vasc. Biol.* **28**, 1050–1059 (2008).
48. P. D. Storer, J. Xu, J. Chavis, P. D. Drew, Peroxisome proliferator-activated receptor-gamma agonists inhibit the activation of microglia and astrocytes: Implications for multiple sclerosis. *J. Neuroimmunol.* **161**, 113–122 (2005).
49. E. Wouters *et al.*, Altered PPARgamma expression promotes myelin-induced foam cell formation in macrophages in multiple sclerosis. *Int. J. Mol. Sci.* **21**, 9329 (2020).
50. T. Fukao, S. Koyasu, PI3K and negative regulation of TLR signaling. *Trends Immunol.* **24**, 358–363 (2003).
51. P. Bascunana, L. Mohle, M. Brackhan, J. Pahnke, Fingolimod as a treatment in neurologic disorders beyond multiple sclerosis. *Drugs R D* **20**, 197–207 (2020).
52. L. J. Scott, Siponimod: A review in secondary progressive multiple sclerosis. *CNS Drugs* **34**, 1191–1200 (2020).
53. K. L. Chan *et al.*, Palmitoleate reverses high fat-induced proinflammatory macrophage polarization via AMP-activated Protein Kinase (AMPK). *J. Biol. Chem.* **290**, 16979–16988 (2015).
54. M. A. Hidalgo, M. D. Carretta, R. A. Burgos, Long chain fatty acids as modulators of immune cells function: Contribution of FFA1 and FFA4 receptors. *Front Physiol.* **12**, 668330 (2021).
55. V. K. Senanayake, W. Jin, A. Mochizuki, B. Chitou, D. B. Goodenowe, Metabolic dysfunctions in multiple sclerosis: Implications as to causation, early detection, and treatment, a case control study. *BMC Neurol.* **15**, 154 (2015).